1.0	4.5	2.8	2.5
	5.0	3.2	2.2
	5.6	3.6	
		4.0	2.0
1.1			
			1.8
1.25	1.4		1.6

MICROCOPY RESOLUTION TEST CHART
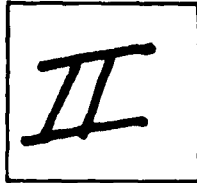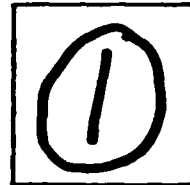NATIONAL BUREAU OF STANDARDS 1963 A

AD A098751

DTIC ACCESSION NUMBER

$\mathbb{II}$

LEVEL

①

INVENTORY

ELECTRON CAPTURE AND IONIZATION CROSS SECTIONS FOR COLLISIONS OF He^{++} WITH Li: PRODUCTION OF He$^+$(3ℓ) AT LOW VELOCITIES*

DOCUMENT IDENTIFICATION

N00014-75-C-0498

DISTRIBUTION STATEMENT A
Approved for public release;
Distribution Unlimited

DISTRIBUTION STATEMENT

ACCESSION FOR
NTIS   GRA&I   ✓
DTIC   TAB   ☐
UNANNOUNCED   ☐
JUSTIFICATION

PER LETTER

BY
DISTRIBUTION /
AVAILABILITY CODES
DIST   AVAIL AND/OR SPECIAL

A

DISTRIBUTION STAMP

DTIC
ELECTE
S   MAY 8   1981   D

B

DATE ACCESSIONED

81   4   27   191

DATE RECEIVED IN DTIC

DTIC FORM OCT 79 70A

DOCUMENT PROCESSING SHEET

R393-010

ELECTRON CAPTURE AND IONIZATION CROSS SECTIONS FOR COLLISIONS OF He^{++} WITH Li: PRODUCTION OF He^{+}(3ℓ) AT LOW VELOCITIES[‡]

E. J. Shipsey, L. T. Redmon, and J. C. Browne
Departments of Physics and Computer Sciences
University of Texas, Austin, Texas 78712

and

R. E. Olson
Molecular Physics Laboratory
SRI International, Menlo Park, California 94025

23 FEBRUARY 1978

ABSTRACT

Single electron capture and ionization cross sections have been calculated for collisions of He^{++} with Li over the relative collision velocity range 0.1-10.0 x 10^{8} cm/sec. For low collision velocities (i.e., v = 0.1-0.6 x 10^{8} cm/sec), a molecular approach has been used to determine the electron capture cross section. Ab initio potential energy curves and coupling matrix elements have been computed for the (HeLi)$^{++}$ system and used in a cross section evaluation based on the perturbed-stationary-state method. For the low velocities, the electron capture reaction He^{++} + Li → He^{+}(3ℓ) + Li^{+} is found to dominate the collision process and proceeds with a large cross section, $\sigma \approx 10^{-15}$ cm^{2}, thus providing the possibility for population inversion and the subsequent emission of Lyman-α (304 Å) and Lyman-β (256 Å) soft x-ray photons. At the higher velocities (i.e., v = 1.4-10.0 x 10^{8} cm/sec), a classical-trajectory Monte-Carlo method has been used to estimate both the electron capture and ionization cross sections. At 2.2 x 10^{8} cm/sec, both cross sections are found to be equal, while one ionization dominates the collision process at higher velocities and electron capture dominates at lower velocities.

81 4 27 191

INTRODUCTION

The search for possible reactions that can give rise to VUV and x-ray radiation has recently centered on charge transfer reactions of multiply charged ions colliding with neutral species. The idea of using electron capture reactions was proposed by Vinogradov and Sobelman[1] and is based on the premise that collisions of the type

$$A^{+q} + B \rightarrow A^{+q-1} + B^{+} \tag{1}$$

preferentially leave the A^{+q-1} product ion in a highly excited electronic state, which subsequently decays to its ground state with the emission of VUV or x-ray photons. The experimental methods needed to utilize reaction (1) to make a superradiant or laser VUV or x-ray light source are very difficult and complex. However, Louisell et al.[2] and Anderson et al.[3] have proposed an experimental setup to make a soft x-ray laser based on reaction (1).

A fundamental issue in the use of reaction (1) to produce an x-ray laser is the specific choice of reactants. Consideration must also be given to the optimum collision velocity for producing a specific electronic level, the possible contamination of lower lying electronic levels that may preclude a population inversion, and whether or not the reaction can be realized experimentally.

One of the first restraints to consider is collision velocity. Generally, for high velocity collisions ($v \gtrsim 2 \times 10^{8}$ cm/sec), the excitation of the A^{+q-1} ion after electron capture tends to be spread over many

electronic levels.[4] Thus, the cross section for producing a specific electronic state is small and the possibility of generating a population inversion is reduced. Also, the charge transfer cross sections decrease rapidly with increasing collision velocity, even when the charge state of A^{+q} is large.[5]

However, even if we restrict ourselves to low velocity collisions, another restraint on the choice of collision partners must be acknowledged. For the more highly charged ions and many electron atomic targets, the reactant state lies in the continuum of the ionization + electron capture process

$$A^{+q} + B \rightarrow A^{+q-1} + B^{++} + e \quad . \tag{2}$$

Hence, we may not only have electron capture to high lying states of A^{+q-1} via (1), but also population of low-lying states of the A^{+q-1} ion via reaction (2), thus removing the possibility of population inversion. Zwally and Koopman[6] very early recognized the importance of process (2) in the analysis of their C^{+4} + Ar cross section data and, more recently, Winter et al.[7] have also shown reaction (2) to be an important process for collisions of multiply charged ions with many electron targets such as Ne and Ar.

Cognizance of the above restraints on the choice of a specific collision system has lead us to search for a reactant combination in which the target atom B is light and the A^{+q} ion is such that it will yield a specific A^{+q-1} electronic level after collision. After surveying

3

many systems using semi-empirical theoretical methods,[8,9] we were lead to

consider a more serious calculation on the $(HeLi)^{++}$ system.

Our present calculations indicate that at low collision velocities

$(v \leqslant 6 \times 10^7$ cm/sec), the electron capture reaction

$$He^{++} + Li \rightarrow He^{+} + Li^{+} \qquad (3)$$

preferentially produces excited $He^{+}(3\ell)$, which will decay either directly to its

ground state with the emission of a 256 $\overset{\circ}{A}$ (48.4 eV) photon or by cascading

via the $He^{+}(2\ell)$ level with the emission of 1640 $\overset{\circ}{A}$ (7.6 eV) and 304 $\overset{\circ}{A}$

(40.8 eV) photons.

Potential energy curves and cross sections for reaction (3) are

presented below. We have used two theoretical methods--a molecular

approach for low velocity collisions and a classical-trajectory Monte-

Carlo method for high velocity collisions--in order to predict the cross

sections for electron capture, reaction (3), and ionization

$$He^{++} + Li \rightarrow He^{++} + Li + e \qquad (4)$$

over the range of velocities $v = 0.1\text{-}10.0 \times 10^8$ cm/sec.

MOLECULAR WAVEFUNCTIONS AND ORBITALS

The wavefunctions for the doublet sigma and pi states are given in

Tables I and II. Each term represents a Slater determinant consisting

of Slater orbitals. The coefficients of minus R in the exponential term

of the Slater orbital are given in Tables III and IV. The orbitals

4

enclosed in parentheses are spin-paired.

There are three charge configurations to account for in the system: $LiHe^{++}$, $Li^{+}He^{+}$, and $Li^{++}He$. The first 12 terms of ψ_{Σ} and the first 6 terms of ψ_{π} correspond to $LiHe^{++}$. Terms 13 through 21 of ψ_{Σ} and terms 7 through 10 of ψ_{π} correspond to $Li^{+}He^{+}$. Finally, the last 7 terms of ψ_{Σ} and the last 2 terms of ψ_{π} account for $Li^{++}He$.

An attempt has been made to achieve the proper spacing of the energy levels in the three systems. "Correlation" terms of the type (1s 1s') and $(2p)^2$ have been included to lower the energy of the more correlated terms of the separated subsystems.   To account for the polarizabilities of the separated subsystems, we have included orbitals that   represent Z times some of the more important atomic orbitals.

The potential curves and coupling elements between the more important states have been computed by means of the computer programs of the Molecular Physics Group of the University of Texas at Austin. The coupling terms computed and inspected for significance include the L_x rotational coupling matrix elements between sigma and pi states with origins at the center of mass, Li atom, and the He atom. The d/dR coupling elements between the sigma states were computed with the origin at the center of mass. The latter computation was performed by differentiating the expansion coefficients in the wavefunction numerically with respect to internuclear separation.

The potential energy curves obtained from our calculations are shown

5

in Fig. 1. We should note that the molecular state Σ_4 correlating to the

$He^{++} + Li$ system crosses the $He^+(3\ell) + Li^+$ manifold at R values ranging

from 33-44 a_o. We have performed Self-Consistent-Field (SCF) calculations to inves-

tigate this outer crossing region and are able to conclude that at the collision

velocities of interest here, the particles proceed diabatically onto the

Σ_4 state. Only for thermal energy collisions will an electron capture

cross section of $\sim 10^{-15}$ cm^2 result from the long range interactions, the

products being $He^+(3\ell) + Li^+$.

There is an avoided crossing between the Σ_4 and Σ_5 states at $R \approx 5.5$ a_o.

Landau-Zener calculations indicate that the probability that the particles will

follow the diabatic potential $(\Sigma_4$ for $R > 5.5$ a_o and Σ_5 for $R < 5.5$ $a_o)$

is close to unity. Hence, for our low velocity cross section evaluation

we need be concerned only with the interactions between Σ_4 for $R > 5.5$ a_o

and Σ_5 for $R < 5.5$ a_o with other close-lying Σ and Π states. From the

computed L_x rotational coupling matrix elements and the d/dR radial coupling

matrix elements, we are able to conclude there is only one significant

interaction: rotational coupling to the Π_2 state whose separated atom

products are $He^+(3p)$ and Li^+. The computed rotational coupling matrix

elements and the potential energy differences between these states are

given in Fig. 2.   We should caution that although

the electron capture proceeds to a state correlating to $He^+(3p) + Li^+$,

long range interactions between all the states arising from $He^+(3\ell) + Li^+$

will considerably distort the product distribution. At this time, we are

unable to predict the specific product distribution among the 3s, 3p, and

3d levels of He^+.

6

CROSS SECTION EVALUATION

A. Low Collision Velocities

The low velocity electron capture cross section evaluations were carried out using the perturbed-stationary-state approximation.[10] In this approximation, the particles follow straight-line classical trajectories while the electronic transitions are treated quantum mechanically. Because of the nature of the $(LiHe)^{++}$ interactions, it is necessary to solve only two coupled equations of the general form:

$$\frac{dc_i(\zeta)}{d\zeta} = - \sum_j \Gamma_{ij}(\zeta) \exp[-i\omega_{ij}(\zeta)] \, c_j(\zeta) \qquad . \qquad (5)$$

In Eq. (5), ζ is related to the impact parameter b and the internuclear separation R by $\zeta^2 = R^2 - b^2$. The interaction potentials V_i arise in (5) as differences via

$$\omega_{ij}(\zeta) = \frac{1}{\hbar v} \int_{-\infty}^{\zeta} (V_j - V_i) \, d\zeta' \qquad , \qquad (6)$$

while the matrix elements for rotational coupling are given by

$$\Gamma_{ij} = \frac{b}{R} L_{ij} \qquad . \qquad (7)$$

The total cross section for a transition from channel i to channel j is then given by

$$Q_j = 2\pi \int_0^\infty db \, b |c_j|^2 \qquad . \qquad (8)$$

Fig. 2 gives the necessary potential difference and rotational coupling matrix element information needed for the cross section evaluation for the electron capture reaction

$$He^{++} + Li \rightarrow He^{+}(3\ell) + Li^{+} \quad . \tag{9}$$
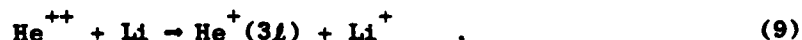
In   Fig. 3 the cross sections for reaction (9) obtained by solving Eqs. (5-8) are shown by   solid circles. The cross sections rise with increasing velocity and are large, $\sigma \approx 10^{-15} \, cm^2$.

Since we have not included electron translational factors in the cross section evaluations, it is not valid to extend the calculations to collision velocities comparable to the orbital velocity v_e of the electron being captured. Hence, for reaction (9) we have restricted our calculations to collision velocities $v \leqslant \frac{1}{2}v_e$, where for a Li atom target, $v_e \simeq 1.4 \times 10^8$ cm/sec.

As a rough estimate of the cross section sensitivity, we have varied the potential differences given in Fig. 2 by $\pm$ 50% and have recalculated the cross sections. The cross sections changed by +60% and -40%, almost linearly with the potential difference change. We have also investigated the effect of changing the origin for the coupling matrix element evaluation from the center-of-mass to origins on the Li or He nucleus. The cross sections varied only slightly with these changes, less than $\pm$ 10%, and hence may be considered   insignificant. Given the probable accuracy of the potential curves relative to one another, our estimate of the cross section accuracy is approximately $\pm$ 50%. However, we do not expect the collision mechanism, that is, production of $He^{+}(3\ell)$, to be changed

by reasonable variations in the potential curves.

B.   High Collision Velocities

For the high velocity collisions, we have   used   a classical-trajectory Monte-Carlo method that has been previously described in detail.[11]   This theoretical method is based on solving Hamilton's equations of motion for a three-particle system.[12]   Basic to the successful application of the method to interactions between charged projectiles and a hydrogenic target is the classical description of the target atom developed by Abrines and Percival.[13]   Percival and Richards[14] have previously argued that the classical-trajectory method will be valid for collision velocities $v \gtrsim v_e$, which for a Li atom target corresponds to $v \gtrsim 1.4 \times 10^8$ cm/sec.

The classical-trajectory method has been successful in predicting the electron capture and ionization cross sections for collisions of multiply-charged ions and atomic hydrogen targets.[11]   For our application to the $(LiHe)^{++}$ system and reactions (3) and (4), it is necessary to describe the Li atom target as an active electron and a point charge for the Li^+ nucleus. We have taken 5.39 eV (the ionization potential for Li) as the energy for the orbital electron and 1.3 as the charge for the Li^+ nucleus. The value of 1.3 is consistent with Slater's rules[15] for the nuclear charge seen by the Li valence electron and is very close to the value of 1.28 obtained by Clementi and Roetti[16] in their optimization of a single zeta basis set for Li.

9

The results of classical-trajectory Monte-Carlo calculations are displayed by   open symbols in Fig. 3. Electron capture dominates the collision process at velocities $v \leqslant 2.2 \times 10^8$ cm/sec, whereas the ionization process dominates at the higher velocities. At the highest velocities we have also investigated the possibility of electron capture or ionization out of the core of the Li atom. No significant contribution was obtained.

As mentioned in the Introduction, the electron capture cross section generally decreases precipitately with increasing velocity when $v \gtrsim 2 \times 10^8$ cm/sec, as shown in Fig. 3. Also, at the higher velocities the electron capture proceeds into a band of electronic levels that broadens with increasing velocity, thus removing the selectivity of the excited electronic states produced. In the classical-trajectory calculations we have monitored this latter behavior by tabulating the energy of the captured electron after collision. At a collision velocity of 1.4×10^8 cm/sec, we find 7% of the electrons are captured in the $n=1$ state of He^+, 46% in $n=2$, 23% in $n=4$, and 6% in $n=5$. With an increase in the collision velocity to 2.2×10^8 cm/sec, this distribution broadens to 7% in $n=1$, 27% in $n=2$, 19% in $n=3$, 13% in $n=4$, and 10% in $n=5$. Hence, at collision velocities $v \gtrsim v_e$, it appears that it will be difficult to realize a population inversion, even though high lying electronic levels of the ion are produced.

10

CONCLUDING REMARKS

Electron capture and ionization cross sections have been calculated

for the He^{++} + Li system over a wide range of collision velocities,

$v = 0.1$-10.0×10^8 cm/sec. At low velocities, $v \leqslant 6 \times 10^7$ cm/sec, the

calculations indicate $He^+(3\ell)$ will be selectively produced during the

collision.   Thus, it appears the He^{++} + Li system

will very efficiently produce soft x-ray photons at wavelengths 256 Å

and 304 Å.

The optimum conditions under which a population inversion could be

attained are also discussed.

It appears that low velocity $v < v_e$ collisions will be most efficient in

this regard, at higher energies the product state distributions tend to

broaden considerably and also the cross section for electron capture

decreases rapidly with increasing velocity. It should be noted,

however, that in low velocity collisions between multiply-charged ions and

many electron target atoms,   the ionization + electron capture process,

reaction (2), will be very important. This process tends to leave the

product A^{+q-1} ion in a low lying excited or ground state, thereby removing

the possibility for population inversion.

REFERENCES

1. A. V. Vinogradov and I. I. Sobelman, Zh. Eksp. Teor. Fiz. 63, 2113
   (1972), [Sov. Phys.-JETP 36, 115 (1973)].

2. W. H. Louisell, M. O. Scully, and W. B. McKnight, Phys. Rev. A 11,
   989 (1975).

3. D. Anderson, J. McCullen, M. O. Scully, and J. F. Seely, Opt. Commun.
   17, 226 (1976).

4. J. A. Guffey, L. D. Ellsworth, and J. R. MacDonald, Phys. Rev. A 15,
   1863 (1977).

5. K. H. Berkner, W. G. Graham, R. V. Pyle, A. S. Schlachter, J. W.
   Stearns, and R. E. Olson, J. Phys. B: Atom. Molec. Phys. (in press).

6. H. J. Zwally and D. W. Koopman, Phys. Rev. A 2, 1851 (1970).

7. H. Winter, E. Bloemen, and F. J. de Heer, J. Phys. B: Atom. Molec.
   Phys. 10, L599 (1977).

8. R. E. Olson, F. T. Smith, and E. Bauer, Appl. Opt. 10, 1848 (1971).

9. R. E. Olson and A. Salop, Phys. Rev. A 14, 579 (1976).

10. D. R. Bates and R. MacCarroll, Proc. Roy. Soc. (London) A245, 175
    (1958).

11. R. E. Olson and A. Salop, Phys. Rev. A 16, 531 (1977).

12. M. Karplus, R. N. Porter, and R. D. Sharma, J. Chem. Phys. 43, 3259 (1965).

13. R. Abrines and I. C. Percival, J. Phys. B: Atom. Molec. Phys. 88, 861 (1966).

14. I. C. Percival and D. Richards, Advances in Atom. Molec. Phys., ed. by D. R. Bates and I. Esterman, Vol. II (Academic Press, New York, 1975), p. 1.

15. H. Eyring, J. Walter, and G. E. Kimball, Quantum Chemistry (John Wiley and Sons, Inc., New York, 1964), p. 162.

16. E. Clementi and C. Roetti, Atom. Data and Nucl. Data Tables 14, 177 (1974).

TABLE I

SIGMA WAVEFUNCTION

$$\Psi_\Sigma = A_1(1S_{Li})^2 2S_{Li} + A_2(1S_{Li})^2 3S_{Li} + A_3(1S_{Li})^2 4S_{Li} + A_4(2p_{Li}^0)^2 2S_{Li}$$

$$+ A_5(2p_{Li}^- 2p_{Li}^+)2S_{Li} + A_6(1S_{Li})^2 3p_{Li}^0 + A_7(1S_{Li})^2 4p_{Li}^0 + A_8(1S_{Li})^2 5p_{Li}^0$$

$$+ A_9(2p_{Li}^0)^2 3p_{Li}^0 + A_{10}(2p_{Li}^- 2p_{Li}^+)3p_{Li}^0 + A_{11}(1S_{Li}\, 2p_{Li}^{0'})2S_{Li} + A_{12}(1S_{Li})^2 2p_{Li}^{0''}$$

$$+ A_{13}(1S'_{Li} 1S''_{Li})1S_{He} + A_{14}(1S'_{Li} 1S''_{Li})1S'_{He} + A_{15}(1S'_{Li} 1S''_{Li})2S_{He}$$

$$+ A_{16}(1S'_{Li} 1S''_{Li})2p_{He}^0 + A_{17}(1S'_{Li} 1S''_{Li})3S_{He} + A_{18}(1S'_{Li} 1S''_{Li})3p_{He}^0$$

$$+ A_{19}(1S'_{Li} 1S''_{Li})3d_{He}^0 + A_{20}(1S'_{Li} 1S''_{Li})4S_{He} + A_{21}(1S'_{Li} 1S''_{Li})4p_{He}^0$$

$$+ A_{22}(1S''_{He} 1S'''_{He})1S'''_{Li} + A_{23}(1S''_{He} 2p_{He}^{0''})1S'''_{Li} + A_{24}(1S'''_{He} 2p_{He}^{0'})1S'''_{Li}$$

$$+ A_{25}(1S_{He} 2p_{He}^{0'''})1S'''_{Li} + A_{26}(1S_{He} 2S_{He})1S'''_{Li} + A_{27}(1S_{He} 1S'''_{Li})2p_{He}^{0'''}$$

$$+ A_{28}(1S_{He} 1S'''_{Li})2S_{He}$$

TABLE II

PI WAVE FUNCTION

$$\Psi_\pi = B_1(1S_{Li})^2 3p^+_{Li} + B_2(1S_{Li})^2 4p^+_{Li} + B_3(2p^o_{Li})^2 3p^+_{Li}$$

$$+ B_4(2p^-_{Li}2p^+_{Li})3p^+_{Li} + B_5(1S_{Li}2p^{+'}_{Li})2S_{Li} + B_6(1S_{Li})^2 2p^{+''}_{Li}$$

$$+ B_7(1S'_{Li}1S''_{Li})2p^+_{He} + B_8(1S'_{Li}1S''_{Li})3p^+_{He} + B_9(1S'_{Li}1S''_{Li})3d^+_{He}$$

$$+ B_{10}(1S'_{Li}1S''_{Li})4p^+_{He} + B_{11}(1S_{He}2p^{+'}_{He})1S'''_{Li}$$

$$+ B_{12}(1S_{He}1S'''_{Li})2p^{+'}_{He}$$

TABLE III

SIGMA ORBITALS

ORBITAL	EXPONENT	ORBITAL	EXPONENT
$1S_{Li}$	2.6864	$1S_{He}$	2.0000
$1S'_{Li}$	3.2949	$1S'_{He}$	1.0000
$1S''_{Li}$	2.0790	$1S''_{He}$	2.1832
$1S'''_{Li}$	3.0000	$1S'''_{He}$	1.1885
$2S_{Li}$	0.6374	$2S_{He}$	
$2p^-_{Li}$		$2p^o_{He}$	1.0000
$2p^o_{Li}$	3.9756	$2p^{o'}_{He}$	2.1832
$2p^+_{Li}$		$2p^{o''}_{He}$	1.1885
$2p^{o'}_{Li}$	2.6864	$2p^{o'''}_{He}$	0.4868
$2p^{o''}_{Li}$	0.5256	$3S_{He}$	
$3S_{Li}$	0.9563	$3p^o_{He}$	0.6667
$3p^o_{Li}$	0.6374	$3d^o_{He}$	
$4S_{Li}$		$4S_{He}$	0.7183
$4p^o_{Li}$	0.9563	$4p^o_{He}$	0.7285
$5p^o_{Li}$			

TABLE IV

PI ORBITALS

ORBITAL	EXPONENT	ORBITAL	EXPONENT
$1S_{Li}$	2.6864	$1S_{He}$	2.0000
$1S'_{Li}$	3.2949	$2p^+_{He}$	1.0000
$1S''_{Li}$	2.0790	$2p^{+'}_{He}$	0.4868
$1S'''_{Li}$	3.0000	$3p^+_{He}$	0.6667
$2S_{Li}$	0.6374	$3d^+_{He}$	0.6667
$2p^-_{Li}$		$4p^+_{He}$	0.7285
$2p^o_{Li}$	4.0144		
$2p^+_{Li}$			
$2p^{+'}_{Li}$	2.6864		
$2p^{+''}_{Li}$	0.5256		
$3p^+_{Li}$	0.6374		
$4p^+_{Li}$	0.9667		

FIGURE CAPTIONS

1. Potential energy curves for the $(HeLi)^{++}$ system. Solid lines denote $^2\Sigma$ molecular states; dashed lines denote $^2\Pi$ molecular states. Note the diabatic potential curves that correlate to the He^{++} + Li reactants, Σ_5 for $R \leq 6.0$ a_o and Σ_4 for $R \geq 6.0$ a_o. These states are coupled strongly via rotational coupling to the Π_2 state which dissociates to $He^+(3p)$ + Li^+.

2. Rotational coupling matrix element and potential energy difference between the Π_2 state of $He^+(3p)$ + Li^+ and the Σ_5 (for $R \leq 6.0$ a_o) and Σ_4 ($R \geq 6.0$ a_o) states which correlated diabatically to the He^{++} + Li reactants.

3. Calculated electron capture cross section for reaction (3) using a molecular approach that is appropriate for low velocity collisions, solid circles, and a classical-trajectory Monte-Carlo approach that is valid for high velocity collisions, open circles. The ionization cross section for reaction (4) calculated using the classical-trajectory Monte-Carlo method is shown by the open triangles.
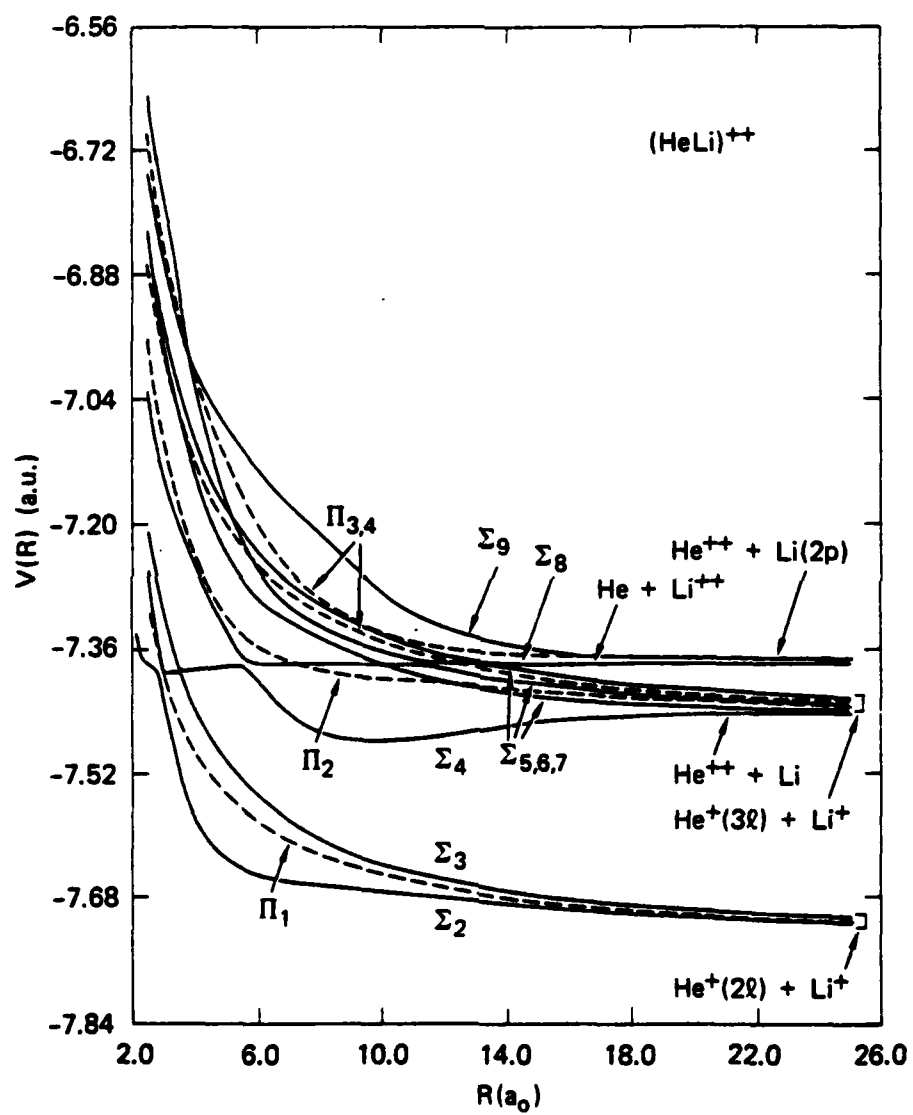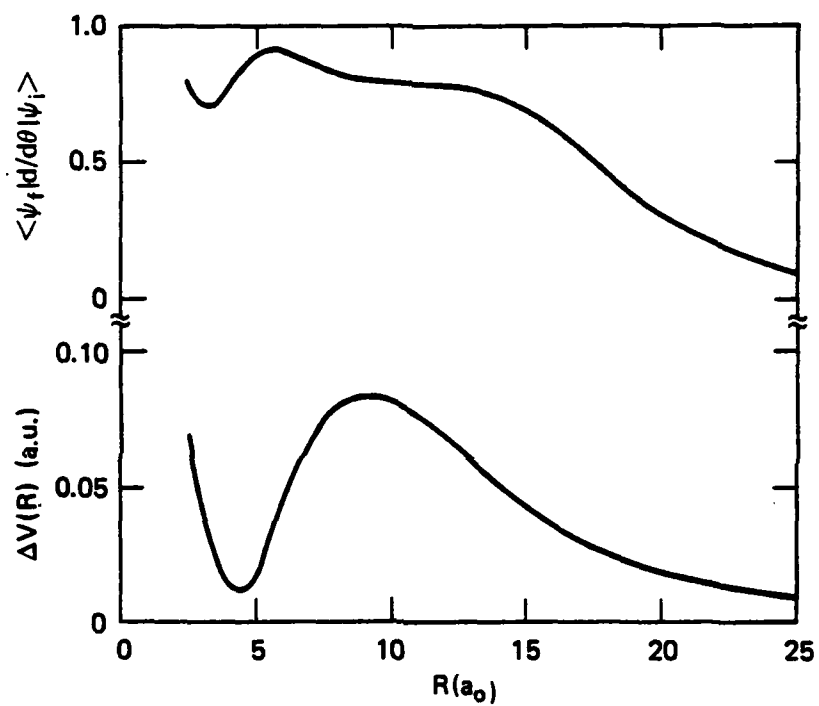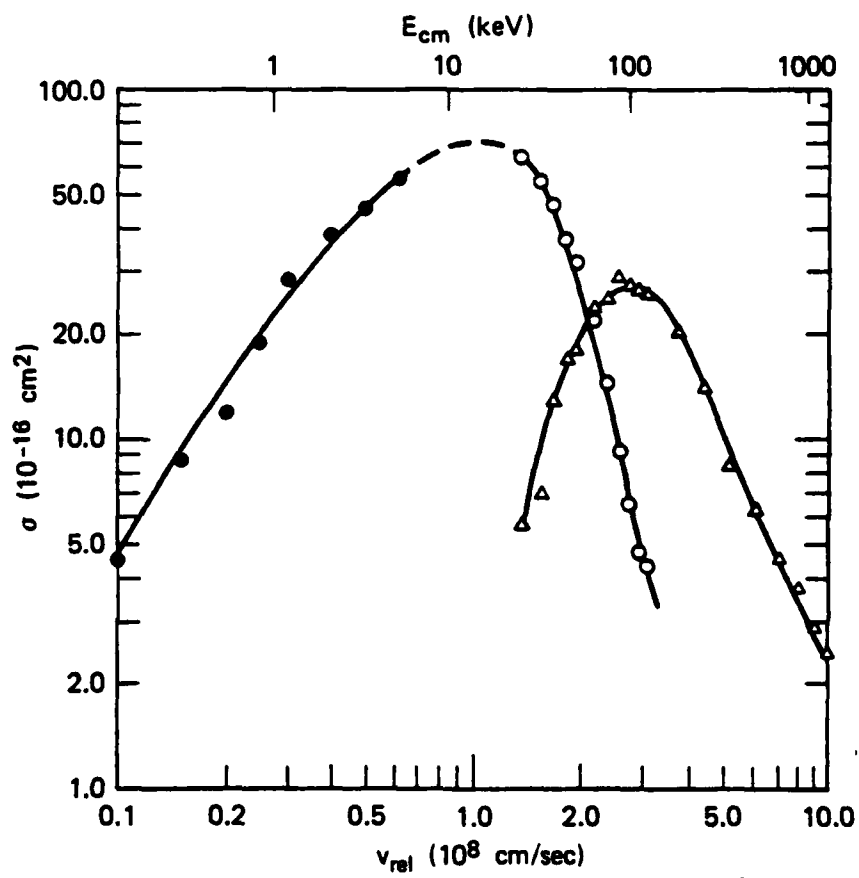
Figure 1

Figure 2

SA-5362-36

Figure 3